Thermal properties of $SmFeAsO_{1-x}F_x$ as a probe of the interplay between electrons and phonons

M. Tropeano,[1] A. Martinelli,[2] A. Palenzona,[2] E. Bellingeri,[1] E. Galleani d'Agliano,[1] T. D. Nguyen,[3] M. Affronte,[3] and M. Putti[1]

[1]*Dipartimento di Fisica, CNR-INFM-LAMIA, Via Dodecaneso 33, 16146 Genova, Italy*

[2]*Dipartimento di Chimica and Chimica Industriale, CNR-INFM-LAMIA, Via Dodecaneso 31, 16146 Genova, Italy*

[3]*Dipartimento di Fisica, Università di Modena e Reggio Emilia, CNR-INFM-S3, Via G. Campi 213/A, I-41100 Modena, Italy*

(Received 4 July 2008; revised manuscript received 1 September 2008; published 26 September 2008)

A comparative study of thermal properties of SmFeAsO, $SmFeAs(O_{0.93}F_{0.07})$, and $SmFeAs(O_{0.85}F_{0.15})$ samples is presented. Specific heat and thermal conductivity show clear evidence of the spin-density wave (SDW) ordering below $T_{SDW} \sim 135$ K in undoped SmFeAsO. At low level of F doping, $SmFeAs(O_{0.93}F_{0.07})$, SDW ordering is suppressed and superconducting features are not yet optimally developed in both specific heat and thermal conductivity. At optimal level of F-doping $SmFeAs(O_{0.85}F_{0.15})$ anomalies related to the superconducting transition are well noticeable. By a compared analysis of doped and undoped samples we conclude that despite the fact that F doping modifies definitely the electronic ground state, it does not substantially alter phonon and electron parameters, such as phonon modes, Sommerfeld coefficient, and electro-phonon coupling. The analysis of the thermal conductivity curves provides an evaluation of the SDW and superconducting energy gap, showing that phonons can suitably probe features of the electronic ground state.

DOI: 10.1103/PhysRevB.78.094518 PACS number(s): 75.30.Fv, 65.40.−b, 71.27.+a, 74.70.−b

I. INTRODUCTION

The recent discovery of superconductivity at critical temperature T_c up to 50 K in layered rare-earth (RE) iron-based oxipnictide compounds REFeAsO (RE=La, Ce, Pr, Nd, Sm) (Refs. 1–4) has sparked enormous interest in this class of materials. Like high-T_c cuprates they have layered structure with conducting FeAs layers sandwiched between insulating REO layers, and exhibit superconductivity at relatively high temperatures upon electron[1–5] or hole doping[6] of the related nonsuperconducting compounds. The latter exhibit a magnetic transition with a sharp drop of resistivity below 140–150 K.[1–3] This anomaly has been explained within controversial theoretical frameworks.[7–14] Optical[7] measurements suggest that LaFeAsO has an antiferromagnetic spin-density-wave (SDW) state. This has been confirmed by neutron scattering studies,[15] which provide evidence for an antiferromagnetic long-range ordering with a small $0.35\mu_B$ per Fe moment below 140 K. Nearly at the same temperature a structural transition has been reported for LaFeAsO,[15] NdFeAsO,[16] and recently for SmFeAsO.[17]

More recently a new class of double layer AFe_2As_2 (A=Sr, Ba, Eu) compounds has been investigated. They present even more pronounced resistivity and specific-heat anomalies at a temperature that ranges from 130 to 200 K, and T_c increases up to 38 K when doped with holes.[18–21]

First-principles calculations indicate that electron-phonon coupling is not sufficient to explain superconductivity.[8,22] On the other hand, thermal properties are strongly affected by the establishment of a SDW,[7,18] suggesting that these properties can be useful tools to investigate details of electronic structure. To our knowledge, an in-depth analysis of thermal properties of oxipnictides is still lacking in the literature.

In this work we report results of specific-heat and thermal conductivity measurements on SmFeAsO, which exhibits anomalies at ~135 K. Although the nature of this anomaly is not yet definitively clear, in the following we refer to it as due to the transition to a SDW ordered state. The same properties measured on $SmFeAs(O_{0.93}F_{0.07})$ show that anomalies at ~135 K are suppressed while the superconducting features are still not well developed. Superconducting anomalies are clearly evident in both specific heat and thermal conductivity of $SmFeAs(O_{0.85}F_{0.15})$. A lambda anomaly is clearly evident in the specific heat of the three samples close to liquid helium temperature. Remarkably, the lattice properties are very close for the three samples and this allows direct comparison of the thermal properties of doped and undoped cases, leading to an evaluation of the SDW and superconducting energy gap. It turns out from this analysis that thermal properties can suitably probe details of the electronic ground state. For the sake of clarity, we focus on the thermal properties of the parent SmFeAsO in comparison with the $SmFeAs(O_{0.93}F_{0.07})$ sample first, and we discuss the superconducting properties of $SmFeAs(O_{0.85}F_{0.15})$ second.

II. EXPERIMENTAL DETAILS

The SmFeAsO, $SmFeAs(O_{0.93}F_{0.07})$, and $SmFeAs(O_{0.85}F_{0.15})$ samples were prepared in three steps as described in Ref. 23: (1) synthesis of SmAs from pure elements; (2) synthesis of SmFeAsO and $SmFeAs(O_{1-x}F_x)$ by reacting SmAs with stoichiometric amounts of Fe, Fe_2O_3, and FeF_2 at high temperature; and (3) grinding of the so-obtained sample and further sintering at high temperature, in order to obtain a compact sample. The samples were characterized by x-ray powder diffraction followed by Rietveld refinement, revealing their single-phase nature. Transmission electron microscopy (TEM) analysis evidences the lack of structural defects. The effect of sintering is to increase the density and connection between the grains, improving substantially the transport properties.

Heat capacity and thermal conductivity were measured by a Quantum Design physical property measurement system (PPMS). Heat-capacity measurements were performed by using the two-tau method.

Resistivity and magnetization measurements reported elsewhere,[23,24] evidence of a pronounced anomaly around

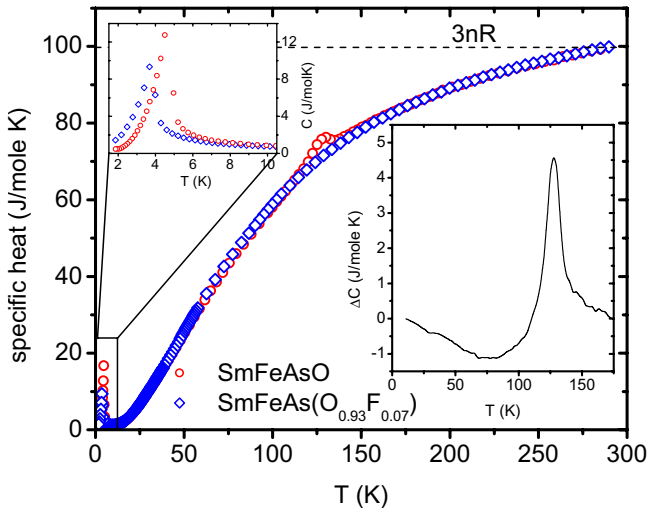

FIG. 1. (Color online) Temperature dependence of the specific heat of SmFeAsO and $SmFeAs(O_{0.93}F_{0.07})$. Upper inset: specific-heat anomaly $\Delta C(T)$ related to the SDW.

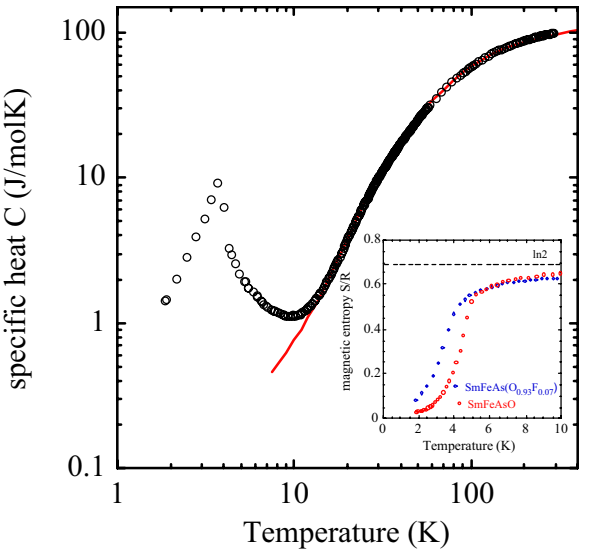

FIG. 2. (Color online) Specific-heat data of $SmFeAs(O_{0.93}F_{0.07})$ and $C(T)=\gamma T+C_D(T)+C_E(T)$ (continuous line). Inset: S_m associated to the ordering of the Sm^{3+} sublattice.

140 K in SmFeAsO specimen. $SmFeAs(O_{0.93}F_{0.07})$ does not reveal the SDW anomaly and shows a rather broad superconducting transition below $T_c \sim 34$ K probably related to the somewhat inhomogeneous distribution of fluorine. $SmFeAs(O_{0.85}F_{0.15})$, instead, undergoes a sharp superconducting transition at $T_c=51.5$ K as detected by resistivity and susceptibility measurements,[24] and exhibits well-developed and sharp anomalies in the thermal properties as discussed below.

III. SDW STATE

A. Specific heat

The temperature dependence of the specific heat C of SmFeAsO is plotted in Fig. 1 and it can be compared to that of $SmFeAs(O_{0.93}F_{0.07})$ and to that of $SmFeAs(O_{0.85}F_{0.15})$ in Fig. 5. Remarkably, the absolute values of C are quite close for the three samples. At high temperature, the C values tend to saturate to the Dulong Petit value $3nR$ with $n=4$ and $R=8.314$ J/mol K—the gas constant. These features lead to the conclusion that fluorine doping induces only little quantitative changes in the lattice, as expected from the almost identical crystalline structure.[23] This result is fully consistent by the phonon density of states measurements in undoped and optimally doped $LaFeAsO_{1-x}F_x$.[25] Our results thus rectify data previously reported by Ding *et al.*[26] for which the specific heat of $SmFeAsO_{1-x}F_x$ largely exceeded the Dulong Petit value and strongly depended on F doping.

The main difference between the two $C(T)$ curves in Fig. 1 is the anomaly clearly visible and peaked at about 130 K in the undoped SmFeAsO sample but not in $SmFeAsO_{0.93}F_{0.07}$. This anomaly was previously observed[7,26] and ascribed to the SDW transition. We can better show this anomaly by evaluating $\Delta C(T)=C(T)_{SmFeAsO}-C(T)_{SmFeAs(OF)}$. This is plotted in the inset of Fig. 1. Its cusp shape suggests an important role of fluctuations above $T_{SDW} \sim 130$ K, and its height—about 5 J/mol K $\Delta C(T)$—becomes negative below 110 K. If we assume that $C_{SmFeAs(OF)}$ approximates the normal state (no SDW order) behavior, qualitatively this implies that the entropy difference between the normal and the gapped states tends to be compensated at T_{SDW} like in the superconducting transition.

Both SmFeAsO and $SmFeAs(O_{0.93}F_{0.07})$ compounds show sharp peaks in $C(T)$ at 4.6 K and 3.7 K, respectively (see the magnification in Fig. 1). In $SmFeAs(O_{0.85}F_{0.15})$ this peak is a bit smeared. Above these peaks, the $C(T)$ curves fit well a dependence $C/T=\gamma+\beta T^2$. In spite of some uncertainty due to the presence of the peaks, the following parameters can be obtained by fitting data between 15 K and 25 K: $\gamma=(42\pm2)$ mJ/mol K^2 and $\beta=(0.36\pm0.04)$ mJ/mol K^4 for SmFeAsO, $\gamma=(44\pm2)$ mJ/mol K^2 and $\beta=(0.35\pm0.04)$ mJ/mol K^4 for $SmFeAs(O_{0.93}F_{0.07})$, and $\gamma=(39\pm2)$ mJ/mol K^2 and $\beta=(0.38\pm0.04)$ mJ/mol K^4

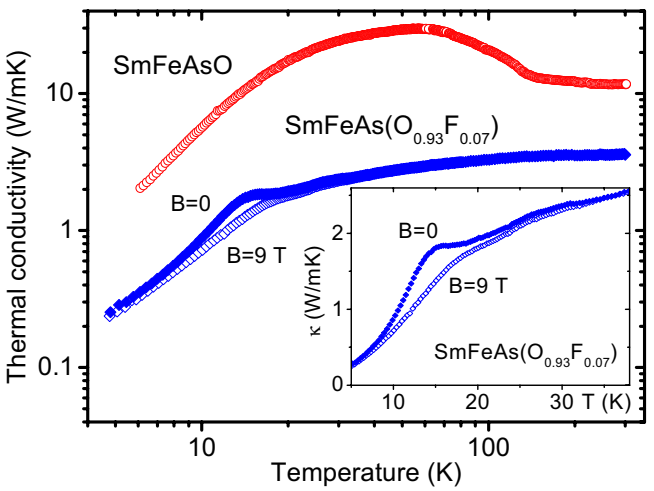

FIG. 3. (Color online) κ of SmFeAsO and $SmFeAs(O_{0.93}F_{0.07})$ as a function of temperature. The inset shows the magnification of the superconducting transition at $B=0$ and $B=9$ T.

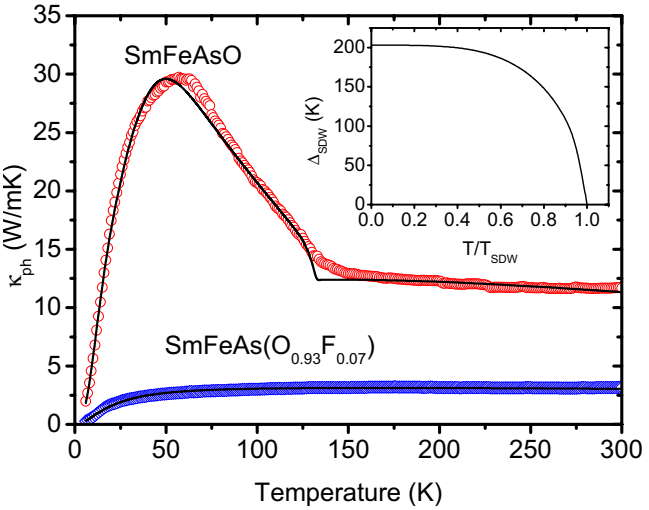

FIG. 4. (Color online) κ_{ph} of SmFeAsO and $SmFeAs(O_{0.93}F_{0.07})$ as a function of temperature. Continuous lines are the best fitting curves evaluated by Eq. (1) with the parameters in Table I. Inset: BCS temperature dependence of the SDW gap.

for $SmFeAs(O_{0.85}F_{0.15})$. It is worth noting that the γ coefficients are similar in doped and undoped samples and are higher (about one order of magnitude) than the Sommerfeld coefficient for the parent compound LaFeAsO.[7,27] Similar values of the γ coefficients were reported for $(Sm_{1.85}Ce_{0.15})CuO_{4-\delta}$,[28] which presents similar layered structure, and the Sm^{3+} sublattice ordinates exactly at the same temperature (4.7 K). The entropy removal related to these peaks can be evaluated as $S_m=\int C_m/T\cdot dT$, where $C_m=C-(\gamma T+\beta T^3)$. For both SmFeAsO and $SmFeAs(O_{0.93}F_{0.07})$, S_m tends to saturate to R ln 2 (see the inset of Fig. 2), as expected for a doublet ground state of Sm^{3+}. This leads us to conclude that the low-temperature peaks can be actually related to the AFM transition of the whole Sm^{3+} sublattice with some little sensitivity to the electron doping. Within this framework, the relatively high γ values might indicate that some hybridization/interaction of the electron wave functions with the Sm^{3+} magnetic ion may lead to renormalization of the effective electron mass. This is supported by resistivity measurements, which show a drop in correspondence of Sm^{3+} AFM transition[23] and by the rather high value of Pauli susceptibility.[24] However, magnetic excitations related to the incipient antiferromagnetic transition of the Sm^{3+} sublattice may also contribute to such high γ values.

The β coefficients are reasonably close for the three compounds and a bit lower than those evaluated for LaFeAsO.[12] In the low-temperature limit, acoustic phonon branches are expected to characterize the lattice vibrations, and the β coefficient can be related to the Debye temperature through the relation $\beta=(12/5)\pi^4R(T/\Theta_D)^3$ from which we can estimate $\Theta_D=175$ K, 173 K, and 170 K for SmFeAsO, $SmFeAs(O_{0.93}F_{0.07})$, and $SmFeAs(O_{0.85}F_{0.15})$, respectively. These rather low Θ_D values well agree with acoustic modes as evaluated in Ref. 22. At higher temperature ($T\geq 30$ K) optical modes contribute as well to the specific heat. By considering optical modes centered at 100 cm^{-1}, 180 cm^{-1}, and 290 cm^{-1} as evaluated in Ref. 22, the overall high-temperature $C(T)$ behavior can be obtained by considering Einstein contributions, C_E, in addition to the Debye, C_D, and the Sommerfeld contributions. This is shown in Fig. 2 where the specific heat of $SmFeAsO_{0.93}F_{0.07}$ above 10 K is well reproduced by the sum of the three contributions $C(T)=\gamma T+C_D(T)+C_E(T)$.

B. Thermal conductivity

In Fig. 3, the thermal conductivity κ of SmFeAsO and $SmFeAs(O_{0.93}F_{0.07})$ is plotted as a function of temperature. The undoped sample presents a clear signature of the SDW transition, abruptly increasing below $T_{SDW}\sim 135$ K. Similar behavior was observed in LaFeAsO,[29] yet the κ values in our case are more than two times higher, indicating good crystallinity of the sample. Measurements at $B=9T$ yield a $\kappa(T)$ curve, not shown for the sake of clarity, that perfectly overlaps data in zero field. This indicates that in the undoped sample mechanisms involved in heat conduction are essentially insensitive to magnetic field.

$SmFeAs(O_{0.93}F_{0.07})$ sample shows thermal conductivity values smaller than those of SmFeAsO and shows very different behavior. In agreement with specific-heat measurements there is no feature around 135 K. Instead maximum occurs around 20 K, as previously observed in Ref. 30. The application of magnetic field reduces thermal conductivity, removing this anomaly. A close data inspection (see the inset) shows that κ(9 T) departs from κ(0 T) below ~34 K, which roughly corresponds to the superconducting critical temperature of this sample.[23]

In LaFeAsO compounds[29,30] it was observed that thermal conductivity is dominated by phonons. This is true also for our samples: by evaluating the electronic contribution $\kappa_e(T)$ by the Wiedemann Franz law ($\kappa_e=L_0T/\rho$, where $L_0=2.45\times 10^{-8}$ W Ω/K and ρ is the resistivity), it actually turns out that $\kappa_e(T)/\kappa(T)$ is less than 1% for SmFeAsO and less than 10% for $SmFeAs(O_{0.93}F_{0.07})$.

From these evaluations it emerges that, independently of the rare-earth and of sample qualities, the heat conduction is

TABLE I. Best fit parameters of the thermal conductivity of SmFeAsO and $SmFeAs(O_{0.93}F_{0.07})$.

Sample	A (W/mK)	Θ_D (K)	η	α	χ	σ_{SDW}
SmFeAsO	0.12(1)	178(2)	9(1)	149(2)	27 (2)	2.90(2)
$SmFeAs(O_{0.93}F_{0.07})$				2240(40)	29 (2)	

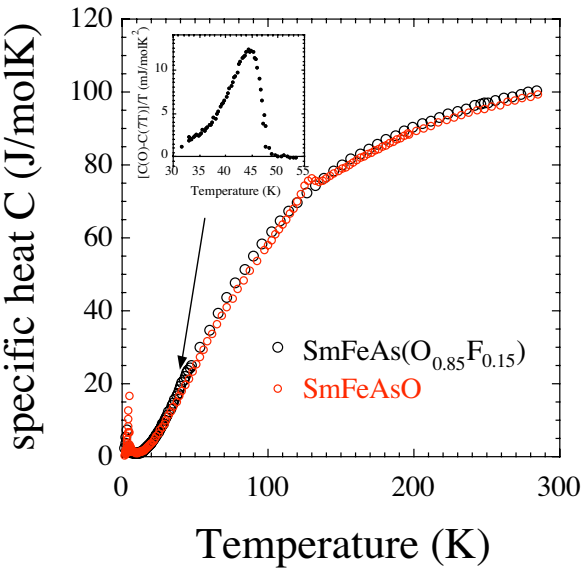

FIG. 5. (Color online) Specific heat of $SmFeAs(O_{0.85}F_{0.15})$ (black circles) as compared with that of SmFeAsO (red circles). Inset: $[C(0)\text{-}C(7T)]/T$ versus temperature.

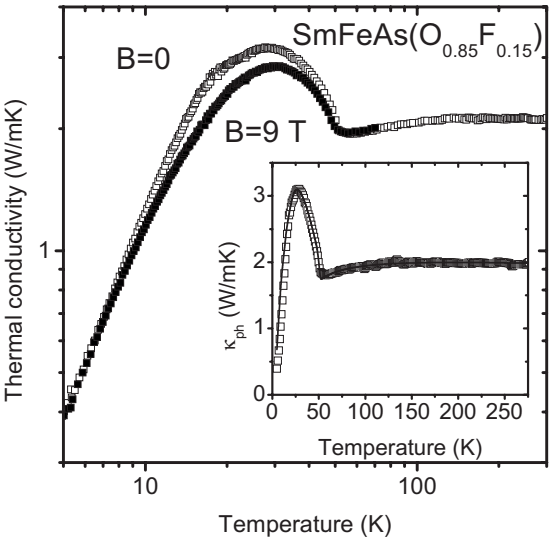

FIG. 6. Thermal conductivity of $SmFeAs(O_{0.85}F_{0.15})$ as a function of temperature at $B=0$ and $B=9$ T. The inset shows κ_{ph} as a function of temperature. Continuous line is the best fit evaluated by Eq. (1) with the parameters in Table II.

dominated by phonons in particular in the sample with low carrier density. Within this framework, an abrupt rise of κ is expected in correspondence to the gap opening at the Fermi surface, followed by carrier condensation and consequent suppression of electron-phonon scattering.

This explains the features observed in Fig. 3: In SmFeAsO, κ rises below T_{SDW}, and in $SmFeAs(O_{0.93}F_{0.07})$ and in $SmFeAs(O_{0.85}F_{0.15})$ (this will be shown in Sec. IV) below T_c. In the case of $SmFeAs(O_{0.93}F_{0.07})$ the application of magnetic field, producing pair breaking, removes nearly completely the anomaly (see the inset of Fig. 3).

For a more quantitative analysis, a phenomenological model that describes the phonon thermal conductivity of superconductors can be used. The model developed initially by Bardeen, Rickayzen, and Tewordt (BRT) in the framework of the BCS theory[31] was later generalized[32] and gives the following expression for the phonon thermal conductivity:[33]

$$\kappa_{ph} = At_D^3 \int_0^{1/t_D} dx \frac{e^x x^4}{(e^x-1)^2} \tau(t_D,x,y), \tag{1}$$

where $t_D = T/\Theta_D$, $x = h\upsilon/k_BT$, and $y = \Delta(T)/k_BT$ are the reduced temperature, phonon energy, and gap energy. Parameter A, assuming that only longitudinal acoustic phonons contribute to κ_{ph}, is approximately[32]

$$A = \left(\frac{4}{3}\pi\right)^{1/3} \frac{k_B^2 L_b}{ha^2} \Theta_D, \tag{2}$$

where a is an average lattice constant and L_b is the typical grain size. $\tau(t_D,x,y)$ is the normalized relaxation time that, according to the Mathiessen rule, may be written as[32]

$$\tau(t_D,x,y)^{-1} = [1 + \alpha t_D^4 x^4 + \chi t_D x g(x,y) + \eta t_D^4 x^2]. \tag{3}$$

The terms proportional to α, χ, and η refer to the main phonon relaxation rates: Point-defects, charge carriers, and other phonons, respectively. Each relaxation rate is divided by the phonon relaxation time with sample boundaries $\tau_b^{-1} = \upsilon_s/L_b$ (υ_s is the sound velocity in the materials). The function $g(x,y)$, which is included in the electron-phonon term, is the ratio between the electron-phonon scattering times in the normal and in the superconducting state, and has been derived in the original BRT theory.[31] The strong similarities existing between superconducting and SDW ground states[34] suggest that the same derivation can be applied here, introducing as a free parameter $\sigma_{SDW} = \Delta_{SDW}(0)/k_BT_{SDW}$ and assuming a BCS temperature dependence of the gap.

In Fig. 4 the phonon contributions to the thermal conductivity, κ_{ph}, of SmFeAsO and $SmFeAs(O_{0.93}F_{0.07})$ are plotted as a function of temperature. κ_{ph} is evaluated as $\kappa_{ph} = \kappa - \kappa_e \approx \kappa - L_0T/\rho$.

In the case of $SmFeAs(O_{0.93}F_{0.07})$, neglecting the superconducting transition, κ_{ph} has been evaluated in the normal state by keeping $\kappa(B=9$ T) and by extrapolating κ_e linearly to zero in the superconducting state. Equation (1) depends on the following set of free parameters: A, Θ_D, α, χ, η, and σ_{SDW}. In order to introduce some constraints, the two curves are simultaneously fitted by keeping A, Θ_D, and η equal for the two samples. Θ_D and η are indeed related to the phonon

TABLE II. Best fit parameters of the thermal conductivity of $SmFeAs(O_{0.85}F_{0.15})$.

Sample	A (W/mK)	Θ_D (K)	η	α	χ	$T_c(K)$	$\sigma = 2\Delta(0)/k_BT_c$
$SmFeAs(O_{0.85}F_{0.15})$	0.13(1)	180(2)	10(2)	4300(300)	20(2)	51.5	3.9(3)

spectrum, which is not affected by doping as shown by specific-heat measurements, and A is related to the grain size which is similar in the two samples.[23] The best fitting curves are plotted in Fig. 4 as continuous lines. They capture the main features giving a quite satisfying agreement. In the case of SmFeAsO the increase below T_{SDW} is well reproduced even if the fluctuations, which make the curve around the transition less stiff are not taken into account. The best fitting parameters are reported in Table I.

Θ_D essentially coincides with the value obtained by low-temperature specific heat. By parameter A an average grain length $L_b \sim 6$ μm can be evaluated by Eq. (2), assuming an average lattice constant $a=5$ Å: this well agrees with the grain size reported in Ref. 23. The different absolute values of the two curves are mainly taken into account by the parameter α, which is more than one order of magnitude higher in $SmFeAs(O_{0.93}F_{0.07})$ than in SmFeAsO. This coefficient is proportional to point defect scattering which is strongly enhanced by F substitutions. The parameter χ is nearly the same in the two samples. For free electrons χ is proportional to the density of state at the Fermi level,[3,22] $N(0)$, thus suggesting that $N(0)$ is substantially unchanged after doping. The same can be concluded by comparing the above reported Sommerfeld γ constant of the two samples. The coefficient χ can be expressed in terms of the longitudinal acoustic phonon contribution to the electron-phonon coupling constant, λ_{la} (Ref. 32): $\chi \approx (\pi/2)(k_B T_{SDW}/\bar{t})(L_b/a)\lambda_{la}$, where $\bar{t} \approx N(0)^{-1}$ is the effective hopping matrix element for a two-dimensional tight-binding band of electrons. With $T_{SDW}=135$ K, $L_b=6$ μm, $a=5$ Å, and $N(0) \sim 2.6-2.1$ states/eV^-,[9,22] we obtain $\lambda_{la} \sim 0.04-0.05$. This value fairly agrees with the estimated contribution of the longitudinal acoustic mode to the total electron-phonon coupling constant as inferred from Ref. 22.

Finally we consider the σ_{SDW} coefficient, which is expected to assume the BCS value 3.52. In our case we evaluated $\sigma_{SDW}=2\Delta_{SDW}(0)/k_B T_{SDW}=2.9$. In the inset of Fig. 4 the temperature dependence of the SDW gap with $\Delta_{SDW}(0)=199$ K$=17$ meV is plotted.

Within a BCS framework the specific-heat anomaly can be evaluated as $\Delta C_{SDW}/\gamma T_{SDW} \approx 1.43(\sigma_{SDW}/3.52)$, where the height of the jump has been scaled with the reduced gap. Assuming $\gamma=42$ mJ/mol K, $T_{SDW}=135$ K, $\sigma_{SDW}=2.9$, we obtain $\Delta C_{SDW} \sim 6.6$ J/mol K, not far from the value of 5 J/mol K experimentally evaluated.

IV. SUPERCONDUCTING STATE.

A. Specific heat

Figure 5 shows the specific heat of $SmFeAsO_{0.85}F_{0.15}$ as compared to that of undoped SmFeAsO. The two $C(T)$ curves essentially overlap each other except in proximity of the respective anomalies: while SmFeAsO shows the SDW bump at 130 K, the specific heat of $SmFeAs(O_{0.85}F_{0.15})$ exhibits a small jump at about 47 K. By subtracting the specific heat $C(7\ \mathrm{T})$ measured in 7 T applied magnetic field, we plot this specific heat jump as $[C(0\ \mathrm{T})-C(T)]/\mathrm{T}$ in the inset of Fig. 5. The jump is relatively sharp and starts at 47 K, and the value at its maximum is $[C(0T)-C(T)]/T=12$ mJ/mol K^2. This is almost twice the values previously reported,[26,35] but it is still less than 0.1% of the absolute specific-heat value. This explains why the anomaly was not observed in not optimally doped and/or not homogeneous samples like $SmFeAs(O_{0.93}F_{0.07})$.[27] Now if we use the $\gamma=39$ mJ/mol K^2, it results in $[C(0\ \mathrm{T})-C(T)]/\gamma T=0.25$, i.e., a value much smaller than what is expected from BCS. This can be partially due to the small inhomogeneity within the sample but it may also indicate that the normal state electronic contribution is overestimated and γ also comprises the contribution from spin excitations related to the antiferromagnetic transition of the Sm^{3+} sublattice as previously mentioned.

B. Thermal conductivity

Figure 6 shows the thermal conductivity κ of $SmFeAs(O_{0.85}F_{0.15})$ as a function of temperature at $B=0$ and $B=9$ T. κ is rather constant at high temperature and abruptly increases below 51 K showing a maximum around 30 K. The application of the magnetic field reduces κ, but the maximum remains well evident. Following step by step the discussion done in the previous section we evaluate that the electron contribution on the thermal conductivity is less than 10%. Thus, also at this level of doping the heat conduction is dominated by phonons and the rise of κ is due to electron condensation below T_c. Different from the case of $SmFeAs(O_{0.93}F_{0.07})$, the application of magnetic field of 9 T does not remove the anomaly, indicating that such a field is much lower than the upper critical field in this sample.

The thermal conductivity of this sample is analyzed within the same theoretical frame introduced in Sec. III B. κ_{ph} versus temperature is plotted in the inset of Fig. 6 where continuous line is the best fit evaluated by Eq. (1) with the parameters listed in Table II. It well reproduces the experimental data with a reasonable set of parameters. A, Θ_D, and ν essentially coincide with the values reported in Table I for SmFeAsO and $SmFeAs(O_{0.93}F_{0.07})$, as expected for similar microstructure and specific-heat values of the three samples. α is nearly two times higher than the value of $SmFeAs(O_{0.93}F_{0.07})$, as expected for a double fluorine content. χ is 30% lower than the values of SmFeAsO and $SmFeAs(O_{0.93}F_{0.07})$, suggesting a decreasing $N(0)$ with increasing doping. Finally the reduced gap value is $2\Delta/k_B T_c=3.9\pm0.3$ from which we evaluate $\Delta(0)=8.5\pm1$ meV. This result is in good agreement with the value obtained by Andreev spectroscopy on $SmFeAs(O_{0.85}F_{0.15})$.[36] We point out, however, that our evaluation assumes a single BCS gap, and it does not consider the occurrence of different pairing symmetries or more energy gaps as recently suggested by some authors.[27,37–41] The inclusion of more complex gap structures in the model could in principle improve the quality of the fit, mainly at low temperature, but it is beyond the purpose of this work.

V. CONCLUSIONS

From the comparative analysis of thermal properties of undoped and F-doped SmFeAsO, two important hints on the nature of the SDW can be drawn:

(1) The SDW transition, evident in both specific heat and thermal conductivity of SmFeAsO, disappears at a low level

of F doping with the occurrence of superconductivity. On the other hand, the phonon structure and, more noteworthy, the electronic density of states are not strongly affected by doping. These results follow by the observation that in the three samples, the lattice specific heat is essentially unchanged, and also the Sommerfeld coefficients γ and the electron-phonon scattering rate parameters χ are nearly equal. This suggests that doping abruptly breaks the symmetries of the Fermi surface inhibiting the SDW formation in favor of superconductivity, without changing substantially both electron and phonon density of states.

(2) The analysis of the thermal properties has emphasized similarities between SDW and a superconducting ground state. The difference between the specific heat of the undoped and doped samples looks qualitatively like the difference between the superconducting and the normal specific heat even if a cusp shape suggests an important role of fluctuations. The thermal conductivity of undoped and optimally doped samples presents similar abrupt rise below the respective ordering temperatures, T_{SDW} and T_c. These behaviors can be well rationalized by describing the SDW transition within a BCS generalized model with $2\Delta_{\mathrm{SDW}}(0)/k_B T_{\mathrm{SDW}} = 2.9$ and the superconducting transition within a BCS single gap model with $2\Delta(0)/k_B T_c = 3.9$.

We conclude that electron-phonon coupling strongly characterizes the thermal properties, giving important clues on the electronic ground states.

ACKNOWLEDGMENTS

This work is partially supported by MIUR under Project No. PRIN2006021741 and by Compagnia di S. Paolo.

[1] Y. Kamihara, T. Watanabe, M. Hirano, and H. Hosono, J. Am. Chem. Soc. **130**, 3296 (2008).
[2] X. H. Chen, T. Wu, G. Wu, R. H. Liu, H. Chen, and D. F. Fang, Nature (London) **453**, 761 (2008).
[3] G. F. Chen, Z. Li, D. Wu, G. Li, W. Z. Hu, J. Dong, P. Zheng, J. L. Luo, and N. L. Wang, Phys. Rev. Lett. **100**, 247002 (2008).
[4] Z. A. Ren, J. Yang, W. Lu, W. Yi, G.-C. Che, X.-L. Dong, L.-L. Sun, and Z.-X. Zhao, Mater. Res. Innovations **12**, 106 (2008).
[5] Zhi-An Ren, Guang-Can Che, Xiao-Li Dong, Jie Yang, Wei Lu, Wei Yi, Xiao-Li Shen, Zheng-Cai Li, Li-Ling Sun, Fang Zhou, and Zhong-Xian Zhao, Europhys. Lett. **83**, 17002 (2008).
[6] H. H. Wen, G. Mu, L. Fang, H. Yang, and X. Y. E. Zhu, Europhys. Lett. **82**, 17009 (2008).
[7] J. Dong, H. J. Zhang, G. Xu, Z. Li, G. Li, W. Z. Hu, D. Wu, G. F. Chen, X. Dai, J. L. Luo, Z. Fang, and N. L. Wang, Europhys. Lett. **83**, 27006 (2008).
[8] I. I. Mazin, D. J. Singh, M. D. Johannes, and M. H. Du, Phys. Rev. Lett. **101**, 057003 (2008).
[9] D. J. Singh and M.-H. Du, Phys. Rev. Lett. **100**, 237003 (2008).
[10] K. Haule, J. H. Shim, and G. Kotliar, Phys. Rev. Lett. **100**, 226402 (2008).
[11] C. Cao, P. J. Hirschfeld, and H. P. Cheng, Phys. Rev. B **77**, 220506(R) (2008).
[12] F. J. Ma and Z. Y. Lu, Phys. Rev. B **78**, 033111 (2008).
[13] T. Yildirim, Phys. Rev. Lett. **101**, 057010 (2008).
[14] Z. P. Yin, S. Lebègue, M. J. Han, B. Neal, S. Y. Savrasov, and W. E. Pickett, Phys. Rev. Lett. **101**, 047001 (2008).
[15] Clarina de la Cruz, Q. Huang, J. W. Lynn, Jiying Li, W. Ratcliff II, J. L. Zarestky, H. A. Mook, G. F. Chen, J. L. Luo, N. L. Wang, and Pengcheng Dai, Nature (London) **453**, 899 (2008).
[16] M. Fratini, R. Caivano, A. Puri, A. Ricci, Zhi-An Ren, Xiao-Li Dong, Jie Yang, Wei Lu, Zhong-Xian Zhao, L. Barba, G. Arrighetti, M. Polentarutti, and A. Bianconi, Supercond. Sci. Technol. **21**, 092002 (2008).
[17] A. Martinelli, A. Palenzona, C. Ferdeghini, M. Putti, and E. Emerich, arXiv:0808.1024 (unpublished).
[18] W. Z. Hu, J. Dong, G. Li, Z. Li, P. Zheng, G. F. Chen, J. L. Luo, and N. L. Wang, arXiv:0806.2652 (unpublished).
[19] Marianne Rotter, Marcus Tegel, and Dirk Johrendt, Phys. Rev. Lett. **101**, 107006 (2008).
[20] Kalyan Sasmal, Bing Lv, Bernd Lorenz, Arnold M. Guloy, Feng Chen, Yu-Yi Xue, and Ching-Wu Chu, Phys. Rev. Lett. **101**, 107007 (2008).
[21] Gen-Fu Chen, Z. Li, G. Li, W. Z. Hu, J. Dong, X. D. Zhang, P. Zheng, N. L. Wang, and J. L. Luo, Chin. Phys. Lett. **25**, 3403 (2008).
[22] L. Boeri, O. V. Dolgov, and A. A. Golubov, Phys. Rev. Lett. **101**, 026403 (2008).
[23] A. Martinelli, M. Ferretti, P. Manfrinetti, A. Palenzona, M. Tropeano, M. R. Cimberle, C. Ferdeghini, R. Valle, M. Putti, and A. S. Siri, Supercond. Sci. Technol. **21**, 095017 (2008).
[24] R. Cimberle, C. Ferdeghini, F. Canepa, M. Ferretti, A. Martinelli, A. Palenzona, A. S. Siri, and M. Tropeano, arXiv:0807.1688 (unpublished).
[25] A. D. Christianson, M. D. Lumsden, O. Delaire, M. B. Stone, D. L. Abernathy, M. A. McGuire, A. S. Sefat, R. Jin, B. C. Sales, D. Mandrus, E. D. Mun, P. C. Canfield, J. Y. Y. Lin, M. Lucas, M. Kresch, J. B. Keith, B. Fultz, E. A. Goremychkin, and R. J. McQueeney, arXiv:0807.3370 (unpublished).
[26] L. Ding, C. He, J. K. Dong, T. Wu, R. H. Liu, X. H. Chen, and S. Y. Li, Phys. Rev. B **77**, 180510(R) (2008).
[27] Gang Mu, Xiyu Zhu, Lei Fang, Lei Shan, Cong Ren, and Hai-Hu Wen, Chin. Phys. Lett. **25**, 2221 (2008).
[28] B. K. Cho, J. H. Kim, Y. J. Kim, Beon-hoan O, J. S. Kim, and G. R. Stewart, Phys. Rev. B **63**, 214504 (2001).
[29] M. A. McGuire, A. D. Christianson, A. S. Sefat, B. C. Sales, M. D. Lumsden, R. Jin, E. A. Payzant, D. Mandrus, Y. Luan, V. Keppens, V. Varadarajan, J. W. Brill, R. P. Hermann, M. T. Sougrati, F. Grandjean, and G. J. Long, arXiv:0806.3878 (unpublished).
[30] Athena S. Sefat, Michael A. McGuire, Brian C. Sales, Rongying Jin, Jane Y. Howe, and David Mandrus, Phys. Rev. B **77**, 174503 (2008).
[31] J. Bardeen, G. Rickayzen, and L. Tewordt, Phys. Rev. **113**, 982 (1959).
[32] L. Tewordt and T. Wolkhausen, Solid State Commun. **70**, 839 (1989); **75**, 515 (1990).
[33] S. Castellazzi, M. R. Cimberle, C. Ferdeghini, E. Giannini, G.

Grasso, D. Marrè, M. Putti, and A. S. Siri, Physica C **273**, 314 (1997).
[34] G. Grüner, Rev. Mod. Phys. **66**, 1 (1994).
[35] C. Senatore, M. Cantoni, G. Wu, R. H. Liu, X. H. Chen, and R. Flukiger, Phys. Rev. B **78**, 054514 (2008).
[36] T. Y. Chen, Z. Tesanovic, R. H. Liu, X. H. Chen, and C. L. Chien, Nature (London) **453**, 1224 (2008).
[37] Lei Shan, Yonglei Wang, Xiyu Zhu, Gang Mu, Lei Fang, Cong Ren, and Hai-Hu Wen, Europhys. Lett. **83**, 57004 (2008).
[38] K. A. Yates, L. F. Cohen, Zhi-An Ren, Jie Yang, Wei Lu, Xiao-Li Dong, and Zhong-Xian Zhao, Supercond. Sci. Technol. **21**, 092003 (2008).
[39] P. Samuely, P. Szabo, Z. Pribulova, M. E. Tillman, S. Bud'ko, and P. C. Canfield, arXiv:0806.1672 (unpublished).
[40] Yonglei Wang, Lei Shan, Lei Fang, Peng Cheng, Cong Ren, and Hai-Hu Wen, arXiv:0806.1986 (unpublished).
[41] R. S. Gonnelli, D. Daghero, M. Tortello, G. A. Ummarino, V. A. Stepanov, J. S. Kim, and R. K. Kremer, arXiv:0807.3149 (unpublished).